

GTEA: Representation Learning for Temporal Interaction Graphs via Edge Aggregation

Yiming Li,¹ Da Sun Handason Tam,¹ Siyue Xie,¹ Xiixin Liu,²
Qiu Fang Ying,² Wing Cheong Lau,¹ Dah Ming Chiu,¹ Shou Zhi Chen²

¹ The Chinese University of Hong Kong

² Tencent Technology Co.Ltd, China

{ly019, tds019, xs019}@ie.cuhk.edu.hk, {xiixinliu, qiufangying}@tencent.com,
{wclau, dmchiu}@ie.cuhk.edu.hk, {easychen}@tencent.com

Abstract

We consider the problem of representation learning for temporal interaction graphs where a network of entities with complex interactions over an extended period of time is modeled as a graph with a rich set of node and edge attributes. In particular, an edge between a node-pair within the graph corresponds to a multi-dimensional time-series. To fully capture and model the dynamics of the network, we propose GTEA, a framework of representation learning for temporal interaction graphs with per-edge time-based aggregation. Under GTEA, a Graph Neural Network (GNN) is integrated with a state-of-the-art sequence model, such as LSTM, Transformer and their time-aware variants. The sequence model generates edge embeddings to encode temporal interaction patterns between each pair of nodes, while the GNN-based backbone learns the topological dependencies and relationships among different nodes. GTEA also incorporates a sparsity-inducing self-attention mechanism to distinguish and focus on the more important neighbors of each node during the aggregation process. By capturing temporal interactive dynamics together with multi-dimensional node and edge attributes in a network, GTEA can learn fine-grained representations for a temporal interaction graph to enable or facilitate other downstream data analytic tasks. Experimental results show that GTEA outperforms state-of-the-art schemes including GraphSAGE, APPNP, and TGAT by delivering higher accuracy (100.00%, 98.51%, 98.05%, 79.90%) and macro-F1 score (100.00%, 98.51%, 96.68%, 79.90%) over four large-scale real-world datasets for binary/ multi-class node classification.

Introduction

In recent years, with the success of deep learning, researchers on graph learning have gradually turned their attention to Graph Neural Networks (GNN). In some previous works, GNNs yield reasonable representations for graphs (Hamilton, Ying, and Leskovec 2017; Veličković et al. 2017) and provide promising results over methods based on shallow embeddings (Grover and Leskovec 2016). By using the spatial construction of graph convolutional filters (Kipf and Welling 2016; Hamilton, Ying, and Leskovec 2017; Veličković et al. 2017), the node embeddings can be computed by iteratively aggregating and transforming neighbors' embeddings. Thus, the local structure of the nodes' can be summarized into low-dimensional vectors. The trained

GNNs can also support inductive learning for unseen graphs with similar types of features.

However, one common limitation of existing GNN models is that the edge features on the graphs are often ignored or poorly supported. One should expect that edge attributes carry information about a pair of adjacent nodes, which can be instrumental in graph learning. Following this intuition, some works (Gong and Cheng 2019; Simonovsky and Komodakis 2017) extend the GNN framework by incorporating both node and edge features of a static graph and result in substantial performance improvement. However, graphs for real-world applications are usually time-evolving, where there can be ongoing interactions between a pair of nodes that define their changing relationships over an extended period of time. One common way to address this problem is to decompose a temporal graph into multiple static graph snapshots by a regular time interval (Yu, Yin, and Zhu 2018; Manessi, Rozza, and Manzo 2020). Some other methods further attempt to yield embeddings that are adaptive to continuous-time space (Xu et al. 2020; Zhang et al. 2020; Kumar, Zhang, and Leskovec 2019).

Although these works have made substantial advances in temporal interaction graph learning, they suffer from the following limitations: **First**, all previous works consider all interactions associated with a node as a single time-series when generating temporal node embeddings. Therefore, they fail to explicitly capture multi-dimensional temporal interaction patterns and relationships for each individual node-pair, which should be beneficial for generating discriminative node representations. Consider the example in Fig. 1 where node *A* is a gambler who has regular betting-related payment interactions with node *C* while behaving normally otherwise with the rest of its neighbors. In this case, the abnormal behavior can be readily captured by modeling the pairwise temporal interactions between node *A* and *C* explicitly, which in turn, helps to identify the role/ illicit activities of these nodes. **Second**, although attention mechanism has been introduced to distinguish different neighbors in some works (Veličković et al. 2017; Xu et al. 2020), a large number of neighbors with small but non-zero attention weight can still overwhelm the few important ones. This is particularly true for real-world applications, e.g., mobile payment networks, where most target nodes do have a large number of (normal) interacting neighbors. This moti-

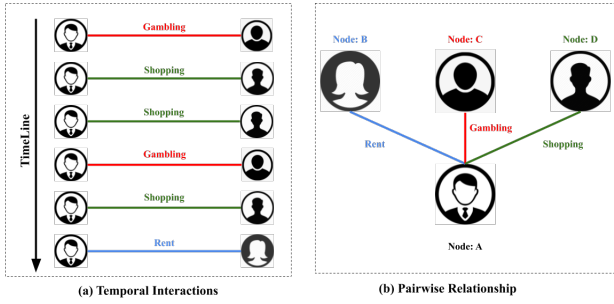


Figure 1: An illustrated example of the motivation of capturing pairwise relationships in a temporal interaction graph. Nodes can have different kinds of interaction events with their neighbors, e.g., node *A* behaves normally with most of its neighbors, while conducting regular gambling activities with node *C*.

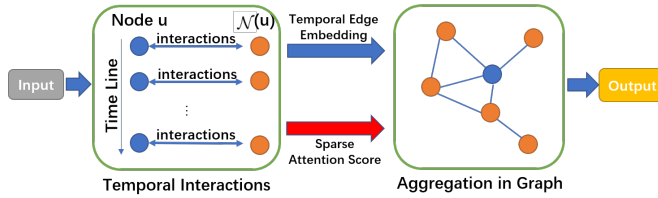


Figure 2: The pipeline of the proposed GTEA framework.

vates the need for filtering out irrelevant neighbors to reduce the effect of noisy information during the learning process. **Third**, some previous work (Zhang et al. 2020) simply concatenate node and edge representations, which holds inferior support to integrate node and edge information as neighbor node embeddings and the corresponding edge embeddings are summed independently during aggregation.

To tackle these challenges, we propose **GTEA** (Graph Temporal Edge Aggregation), a framework of representation learning for temporal interaction graphs. The pipeline of GTEA is depicted in Fig. 2, under which a sequence model is first introduced to learn the temporal dynamics of pairwise nodal interactions. As a result, a low-dimensional edge embedding is generated to encode the temporal interaction patterns between different node pairs. Topological dependencies and relationships among different nodes are then captured through the GNN-based backbone, which incorporates both node features and the learned edge embeddings. To filter out irrelevant information, a sparsity-inducing self-attention mechanism is used when conducting graph neighborhood aggregations. The entire model can be trained end-to-end and all proposed modules are jointly optimized to yield discriminative representations for node classification tasks. We have implemented multiple variants of different sequence models for GTEA and experimental results on four large-scale real-world datasets demonstrate the effectiveness, scalability and state-of-the-art performance of GTEA by conducting binary and multi-class node classifications.

Related Work

In recent years, the development of graph learning has been well propelled by Graph Neural Network (GNN), which achieve great success in tasks including node classification, clustering, link prediction, etc. (Kipf and Welling 2016; Hamilton, Ying, and Leskovec 2017; Veličković et al. 2017). However, real-world graphs are typically time-evolving with node and edge attributes, which can be informative for graph representation learning but usually separately processed by previous works.

EGNN (Gong and Cheng 2019) constructs a weighted graph for each edge features’ dimension. Node embeddings of each weighted graph are obtained by applying a GCN model and they are concatenated together to form the final node embeddings of the original graph. As such, edge features are only regarded as connectivity/ aggregation weights for nodes. ECCConv (Simonovsky and Komodakis 2017) uses a filter generating network which takes multiple edge features as input and generates a set of edge-specific weights for the GCN. Although different patterns can be learned through the model, the dense filter in ECCConv can result in huge memory consumption, which hinders its scalability with large graphs.

One common way to handle temporal graphs is to decompose it into multiple static graph snapshots by a regular time interval (Yu, Yin, and Zhu 2018; Singer, Guy, and Radinsky 2019). DCRNN (Li et al. 2018) embeds the graph convolution into the LSTM model, which learns to capture relational dependencies within a period of time. EvolveGCN (Pareja et al. 2020) utilizes RNN-based variants to generate different GCN weights for each snapshot, which learns to extract different relational patterns at different time. However, a sequence of graph snapshots is a coarse approximation of the continuous time-evolving graph in the real-world. This results in quantization and temporal information loss as it groups all data within a time interval into a single static graph. In addition, the setting of regular time interval prevents these models from learning relational patterns with different time-scales, which makes it hard to capture variable interactional relationships of a node pair across time. Such drawbacks prevent them from generalizing to more complicated temporal interaction graphs.

Instead of learning from graph snapshots, JODIE (Kumar, Zhang, and Leskovec 2019) uses two recurrent neural networks to update node embeddings in each interaction. (Zhang et al. 2020) further utilizes the edge features to enhance the representation of nodes. TGAT (Xu et al. 2020) adopts a continuous-time kernel encoder with a self-attention layer to aggregate interactions among neighbors. Know-Evolve (Trivedi et al. 2017) and DyRep (Trivedi et al. 2018) learn evolving entity representations on temporal knowledge graphs using temporal point process. However, all models treat the interactions between a target node and all of its neighbors as one single time-series, which makes it difficult for the model to learn relational patterns that are specific to individual node-pairs. Different from the aforementioned works, our proposed model learns the temporal interaction patterns for each specific node pair, which leads to a more fine-grained pairwise nodal relationship modeling

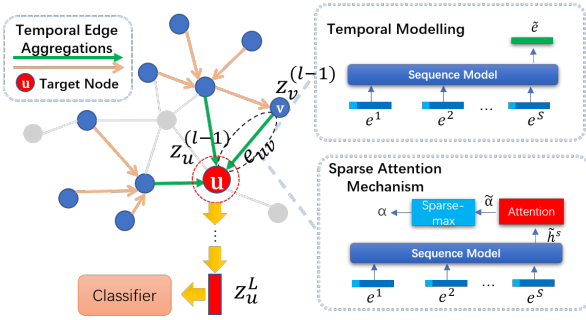


Figure 3: The framework of the proposed GTEA. For a pair of nodes, temporal dynamics are built through a sequence model, which yields a fine-grained temporal edge embedding. Besides, we apply one more sequence model with sparse attention mechanism to catch important temporal behaviors. The learned edge embeddings will be aggregated together with nodes attributes recursively and finally generate a discriminative representation for each node, which can be generalized to some downstream tasks, e.g., node classification.

for temporal interaction graphs.

The GTEA Framework

Problem Formulation

Definition: a **Temporal Interaction Graph** is an attributed graph $\mathcal{G} = (\mathcal{V}, \mathcal{E})$ where \mathcal{V} is the set of vertices and \mathcal{E} is a set of edges. Let $N = |\mathcal{V}|$ be the total number of vertices and $M = |\mathcal{E}|$ be the total number of edges. $\mathcal{N}(u)$ stands for the set of neighbors that node u interacts with. Let $x_u \in \mathbb{R}^{D_N}$ be the feature vector of node u with D_N dimension. An edge (u, v) in \mathcal{E} corresponds to a sequence of interaction events between node u and v taking over an extended period of time. The k -th interaction event between u and v occurs at time t_{uv}^k and is represented by $\mathbf{e}_{uv}^k = (t_{uv}^k, \mathbf{f}_{uv}^k)$ where $\mathbf{f}_{uv}^k \in \mathbb{R}^{D_E}$ is a D_E -dimension event feature-vector. Let S_{uv} be the number of interaction events between node u and v with $t_{uv}^1 \leq t_{uv}^2 \dots \leq t_{uv}^{S_{uv}}$.

Our definition of temporal interaction graph is similar to that of (Zhang et al. 2020) except that we also consider node features and the graphs of interest are not restricted to be bipartite. In contrast to the temporal graphs in (Yan, Xiong, and Lin 2018), which contain a sequence of graph snapshots with only node features, our model considers temporal interactions that take place over continuous time and supports graphs with multi-dimensional node and edge attributes.

Learning Edge Embedding via Sequence Model

To capture the temporal pattern and relationship of the interactions between a pair of nodes, we propose to use state-of-the-art sequence models, including LSTM, Transformer and their time-aware variants, to generate the edge embeddings for a temporal interaction graph. The pairwise nodal interactions are viewed as a time-series that will be fed into the sequence model. For the node pair (u, v) , we denote $\tilde{\mathbf{e}}_{uv}$ as the

edge embedding generated by the sequence model named M_t , where:

$$\tilde{\mathbf{e}}_{uv} = M_t([\mathbf{e}_{uv}^1, \dots, \mathbf{e}_{uv}^{S_{uv}}]). \quad (1)$$

Temporal Dynamics Modeling with LSTM We apply LSTM model (Hochreiter and Schmidhuber 1997) to characterize the interactions between a pair of nodes. The full LSTM model can be described as follows (where we drop the subscript (uv) for notational convenience):

$$\begin{aligned} \mathbf{i}[k] &= \sigma(\mathbf{W}_i \mathbf{e}^k + \mathbf{U}_i \mathbf{h}[k-1] + \mathbf{b}_i) \\ \mathbf{f}[k] &= \sigma(\mathbf{W}_f \mathbf{e}^k + \mathbf{U}_f \mathbf{h}[k-1] + \mathbf{b}_f) \\ \bar{\mathbf{c}}[k] &= \tanh(\mathbf{W}_c \mathbf{e}^k + \mathbf{U}_c \mathbf{h}[k-1] + \mathbf{b}_c) \\ \mathbf{c}[k] &= \mathbf{f}[k] \odot \mathbf{c}[k-1] + \mathbf{i}[k] \odot \bar{\mathbf{c}}[k] \\ \mathbf{o}[k] &= \sigma(\mathbf{W}_o \mathbf{e}^k + \mathbf{U}_o \mathbf{h}[k-1] + \mathbf{b}_o) \\ \mathbf{h}[k] &= \mathbf{o}[k] \odot \tanh(\mathbf{c}[k]) \end{aligned}$$

For the temporal interaction sequences between edge (u, v) , \mathbf{e}^k represents the current input of the LSTM. $\mathbf{i}[k]$, $\mathbf{f}[k]$, and $\mathbf{o}[k]$ denote as state vectors of input gates, forget gates and output gates respectively, while $\mathbf{c}[k]$ is the memory cell and $\mathbf{h}[k]$ is the hidden state. σ and \tanh represent the sigmoid and hyperbolic tangent activation functions respectively. $\mathbf{W}_i, \mathbf{W}_f, \mathbf{W}_c, \mathbf{W}_o, \mathbf{U}_i, \mathbf{U}_f, \mathbf{U}_c, \mathbf{U}_o, \mathbf{b}_i, \mathbf{b}_f, \mathbf{b}_c, \mathbf{b}_o$ are trainable parameters, which are shared for all node-pairs in the network. We take the last hidden output $\mathbf{h}_{uv}[S]$ of the LSTM as the edge embeddings $\tilde{\mathbf{e}}_{uv}$.

Temporal Dynamics Modeling with Transformer Apart from LSTM, Transformer is another popular architecture for sequence modeling, under which sequential, hard-to-parallelize computation during training and inference can be greatly reduced. The key component of the transformer architecture is the self-attention mechanism where a self-attention function maps a query and a set of key-value pairs to an output. In particular, the ‘‘Scaled Dot-Product Attention’’ function can be defined as:

$$\text{Attention}(\mathbf{Q}, \mathbf{K}, \mathbf{V}) = \text{softmax}\left(\frac{\mathbf{Q}\mathbf{K}^T}{\sqrt{D_E}}\right)\mathbf{V}$$

where $\mathbf{Q}, \mathbf{K}, \mathbf{V}$ denotes queries, keys and values matrix, respectively. Given a pair of nodes (u, v) , we denote the event matrix by: $\mathbf{E}_{uv} = [\mathbf{e}^1, \dots, \mathbf{e}^S]^T$. Then the queries, keys and values matrix can be computed as: $\mathbf{Q} = \mathbf{E}_{uv} \mathbf{W}_Q$, $\mathbf{K} = \mathbf{E}_{uv} \mathbf{W}_K$, $\mathbf{V} = \mathbf{E}_{uv} \mathbf{W}_V$, (i.e. they are the projection of \mathbf{E}_{uv}). With the self-attention layer, the edge embeddings $\tilde{\mathbf{e}}_{uv}$ of the edge (u, v) is given by the S -th row of the matrix $\text{Attention}(\mathbf{Q}, \mathbf{K}, \mathbf{V})$.

Temporal Dynamics Modeling with Irregular Temporal Encoding

One drawback of using existing sequence models, e.g., vanilla LSTM or Transformer, as in the previous two subsections, is that it cannot handle irregular time-series. In real-world applications, the interaction sequence between any pair of users are irregular in nature, namely, the update interval between events is not fixed. In this work, in order to learn edge embedding in irregular and continuous time-space, we consider integrating state-of-the-art sequence models with the recent time representation learning

method - Time2Vec (Mehran Kazemi et al. 2019) (**T2V**). For any given time t , we will generate its time embeddings (denoted as **T2V**(t) $\in \mathbb{R}^{(l+1)}$) as follows:

$$\mathbf{T2V}(t)[i] = \begin{cases} \omega_i t + \varphi_i, & \text{if } i = 0. \\ \cos(\omega_i t + \varphi_i), & \text{if } 1 \leq i \leq l. \end{cases} \quad (2)$$

where $\omega'_0, \dots, \omega'_l$ and $\varphi'_0, \dots, \varphi'_l$ are trainable parameters.

On the theoretical side, **T2V** can also be viewed as an extension of Random Fourier Features (RFF) (Rahimi and Recht 2008). If we define $\gamma(t) = \sqrt{\frac{2}{k}}[\cos(\omega'_1 t + \varphi'_1) \dots \cos(\omega'_k t + \varphi'_k)]^\top$ where $\omega'_1, \dots, \omega'_k$ are iid samples from some probability distribution $p(\omega)$ and $\varphi'_1, \dots, \varphi'_k$ are iid samples from the uniform distribution on $[0, 2\pi]$. Then, as a consequence of the Bochner's theorem from harmonic analysis, it can be shown that $\mathbb{E}[\gamma(t_1)^\top \gamma(t_2)] = \phi(t_1, t_2)$ for some positive definite shift-invariant kernel $\phi(t_1, t_2) = \phi(t_1 - t_2)$. Thus, **T2V** can be regarded as RFF with tunable phase-shifts and frequencies. It is worth noting that sinusoidal activation is also found to be suited for representing complex natural signals (Sitzmann et al. 2020) with high precision. In addition, sinusoidal functions with fixed frequencies and phase-shifts have also been used in the Transformer model (Vaswani et al. 2017) as positional encodings. However, it has been shown that learning the frequencies and phase-shifts as in **T2V** rather than fixing them achieves higher performance. By using **T2V**(t) instead of t , Eq. (1) can be extended as follows:

$$\begin{aligned} \tilde{\mathbf{e}}_{uv} &= M_t([\mathbf{e}_{uv}^1, \dots, \mathbf{e}_{uv}^{S_{uv}}]) \\ &= M_t([\mathbf{f}_{uv}^1 || \mathbf{T2V}(t_{uv}^1), \dots, \mathbf{f}_{uv}^{S_{uv}} || \mathbf{T2V}(t_{uv}^{S_{uv}})]) \end{aligned} \quad (3)$$

Sparsity-Inducing Attention Mechanism

In practice, each target node can interact with many neighbors but only a few of them are involved in interactions that are of interest, while other interactions are routine or irrelevant to our data analytic task. To distinguish significant behaviors from non-interesting activities, such as the detection of illicit behaviors within an E-payment network, we adopt another sequence model denoted by M_a with a sparse self-attention mechanism to learn attention scores which reflect the importance of temporal interactions with each individual neighbors of a target node. Neighbors with relatively low attention scores will be filtered out during the GNN-based neighborhood aggregation. Formally, for the edge between node u and node v , let $\tilde{\mathbf{h}}_{uv}$ be the output of the sequence model and apply the self-attention mechanism with a trainable weight vector \mathbf{a} .

As in (Veličković et al. 2017), one can use the softmax function to normalize the attention score across the neighbors of a target node u in the graph. However, softmax can result in many small but non-zero attention weights. If the target node interacts with many neighbors and most of them are irrelevant, those small but non-zero attention values can result in considerable noises during attention-based neighborhood aggregation. To further reduce such noises, we adopt the Sparsemax transformation proposed by (Martins and Astudillo 2016) to obtain a sparse attention-weight

Algorithm 1 Sparsemax Transformation

- 1: **Input:** \mathbf{z}
 - 2: Sort \mathbf{z} as $z_{(1)} \geq \dots \geq z_{(K)}$
 - 3: Find $k(\mathbf{z}) := \max\{k \in [K] | 1 + kz_{(k)} \geq \sum_{j \leq k} z_{(j)}\}$
 - 4: Define $\tau(\mathbf{z}) = \frac{\sum_{j \leq k} z_{(j)} - 1}{k(\mathbf{z})}$
 - 5: **Output:** \mathbf{p} s.t. $p_i = [z_i - \tau(\mathbf{z})]_+$
-

vector. The operation of sparsemax are shown in Algorithm 1, where $[x]_+$ represents the following function:

$$[x]_+ = \begin{cases} x & x > 0 \\ 0 & x \leq 0 \end{cases} \quad (4)$$

After the Sparsemax transformation, unimportant neighbors will be assigned attention scores with zero value and make no contribution to the neighborhood aggregation.

$$\tilde{\mathbf{h}}_{uv} = M_a([\mathbf{e}_{uv}^1, \dots, \mathbf{e}_{uv}^{S_{uv}}]) \quad (5)$$

$$\tilde{\alpha}_{uv} = \mathbf{a}^\top \tilde{\mathbf{h}}_{uv} \quad (6)$$

$$\alpha_{uv} = \text{sparsemax}_v(\tilde{\alpha}_{uv}) \quad (7)$$

Node Representation with Edge Aggregation

To obtain an expressive node representation, we integrate edge embeddings with neighbor node embeddings. (Xu et al. 2020; Zhang et al. 2020) simply concatenate the node embedding with the edge embedding. However, as shown in Equation (8), the weight matrix can be split into two different matrices $W = [W_1, W_2]$.

$$\begin{aligned} \mathbf{z}_{\mathcal{N}(u)}^{(l)} &= \sum_{v \in \mathcal{N}(u)} \mathbf{W}([\mathbf{z}_v^{(l-1)} || \tilde{\mathbf{e}}_{uv}]) \\ &= \mathbf{W}_1 \sum_{v \in \mathcal{N}(u)} \mathbf{z}_v^{(l-1)} + \mathbf{W}_2 \sum_{v \in \mathcal{N}(u)} \tilde{\mathbf{e}}_{uv} \end{aligned} \quad (8)$$

Thus applying naive concatenation cannot have good integration of node and edge embedding because the neighbor node embeddings and corresponding edge embeddings are summed independently (Li, Zhang, and Song 2019). We propose to apply nonlinear activation function, e.g., a Multilayer Perceptron after the concatenation to address this problem. Specifically, the node embedding of any given node $u \in \mathcal{V}$ at layer l , denoted by $\mathbf{z}_u^{(l)}$ is defined recursively as follows:

$$\mathbf{z}_{\mathcal{N}(u)}^{(l)} = \sum_{v \in \mathcal{N}(u)} \alpha_{uv} \text{MLP}_1([\mathbf{z}_v^{(l-1)} || \tilde{\mathbf{e}}_{uv}]) \quad (9)$$

$$\mathbf{z}_u^{(l)} = \text{MLP}_2([\mathbf{z}_u^{(l-1)} || \mathbf{z}_{\mathcal{N}(u)}^{(l)}]) \quad (10)$$

Equation (9) applies attention weighted sum to aggregate both the node embeddings $\mathbf{z}_u^{(l-1)}$ of its neighbors at layer $(l-1)$ and the associated edges representation vector $\tilde{\mathbf{e}}_{uv}$. After computing the neighboring feature vectors $\mathbf{z}_{\mathcal{N}(v)}^{(l)}$, we concatenate it with the target node's embeddings in the previous layer $\mathbf{z}_v^{(l-1)}$ and feed it through another Multilayer Perceptron MLP_2 as in Equation (10).

Algorithm 2 Node Classification using GTEA

Require: Graph $\mathcal{G} = (\mathcal{V}, \mathcal{E})$; node features $x_u, \forall u \in \mathcal{V}$; temporal edge sequences $e_{uv}, \forall (u, v) \in \mathcal{E}$; depth of GCN module L ; aggregation functions MLP_1 and MLP_2 ; neighborhoods of node u : $\mathcal{N}(u)$; sequence model M_t and M_a ; trainable attention weights \mathbf{a}

Ensure: Classification result of node u ;

```
1:  $\mathbf{z}_u^{(0)} \leftarrow x_u$ ;  
2: for  $l = 1, 2, \dots, L$  do  
3:    $\tilde{\mathbf{e}}_{uv} \leftarrow M_t(e_{uv}), \forall v \in \mathcal{N}(u)$ ;  
4:    $\tilde{\mathbf{h}}_{uv} \leftarrow M_a(e_{uv}), \forall v \in \mathcal{N}(u)$ ;  
5:    $\tilde{\alpha}_{uv} \leftarrow \mathbf{a}^\top \tilde{\mathbf{h}}_{uv}$   
6:    $\alpha_{uv} \leftarrow \text{sparsemax}_v(\tilde{\alpha}_{uv})$   
7:    $\mathbf{z}_{\mathcal{N}(u)}^{(l)} \leftarrow \sum_{v \in \mathcal{N}(u)} \alpha_{uv} \text{MLP}_1([\mathbf{z}_v^{(l-1)} || \tilde{\mathbf{e}}_{uv}])$ ;  
8:    $\mathbf{z}_u^{(l)} \leftarrow \text{MLP}_2([\mathbf{z}_u^{(l-1)} || \mathbf{z}_{\mathcal{N}(u)}^{(l)}])$   
9: end for  
10:  $y_u \leftarrow \text{softmax}(\mathbf{z}_u^{(L)})$ ;  
11: return  $y_u$ ;
```

Loss Function

By combining the GCN module and the pairwise temporal sequence model, we can recursively stack the framework at a depth of L layers. We use the standard Cross-entropy loss to drive the end-to-end training of the entire pipeline:

$$\mathcal{L} = - \sum_{l \in \mathcal{Y}_L} \mathbf{y}_l^T \ln(\text{softmax}(\mathbf{z}_l^{(L)}))$$

where \mathcal{Y}_L denotes the set of node indices that have labels and \mathbf{y}_l denotes the one-hot representation of the ground-truth label. We summarize the workflow of GTEA framework in Algorithm 2.

Experiments

In this section, we evaluate the performance of GTEA using four large-scale real-world datasets whose statistics are summarized in Table 1. Experiments are performed to answer the following five questions:

1. How effective is GTEA in binary/ multi-class node classification for temporal interaction graphs?
2. To what extent can GTEA automatically learn from temporal edge features to improve the classification performance?
3. Does the modeling of pairwise nodal interactions/ relationships benefit node classification tasks?
4. How much improvement can the sparsity-inducing attention mechanism achieve over the softmax operation?
5. Is it possible for GTEA to achieve high classification performance without the help of handcrafted or derived interaction/ topology-related node features?

Datasets

Experiments are conducted on Ethereum-Role Dataset (Eth-Role), Ethereum Phishing Large Dataset (Phishing-Large),

Ethereum Phishing Large Dataset (Phishing-Small) and Mobile Payment Network Dataset (Mobile-Payment).

Eth-Role is a multi-class role classification dataset based on the Ethereum Smart Contract network. Unlike Bitcoin, the address in Ethereum is an account that can be used repeatedly. We collect Ethereum transactions by using Google BigQuery and ground truth labels are collected from: <https://etherscan.io>. **Phishing-Large** and **Phishing-Small** are collected from Ethereum Phishing Datasets¹, which is provided by (Chen et al. 2019). Binary classification is conducted on these two datasets to detect phishing accounts in the Ethereum payment network. **Mobile-Payment** is collected from a major mobile payment provider. Models should conduct binary classification to identify abnormal users in the payment network. To build the graph, each account/ user is taken as a node and transaction sequences between two nodes indicate an edge. Detailed descriptions of datasets can be found in the supplementary materials.

Baselines and Variants

To evaluate the performance of GTEA, we compare our model with state-of-the-art GNN methods that are able to handle large-scale graphs. Different variants of advanced sequence modeling approaches have been implemented under the GTEA framework for comparison. Specifically, there are eight baseline models and five GTEA variants, which can be categorized as follows:

- **Models without graph topology.** In this group, we choose XGBoost (Chen and Guestrin 2016), which only uses node features without explicitly considering the graph topology.
- **GNN with only node features.** These methods are state-of-the-art GNN that learn node embeddings based on node features. We take GCN(Kipf and Welling 2016), GraphSAGE (Hamilton, Ying, and Leskovec 2017), GAT (Veličković et al. 2017), and APPNP(Klicpera, Bojchevski, and Günnemann 2018) as the representative schemes for comparison.
- **GNN incorporates edge features.** This category of models incorporates node features as well as statistical edge features that are manually derived from temporal interactions between each node pair. We choose EConv(Simonovsky and Komodakis 2017) and EGNN(Gong and Cheng 2019) as representatives for comparison. We also implement another variant of GTEA named GTEA-ST, which replaces the automatically learned edge-embedding with handcrafted interaction-statistics-based features, including the averaged, minimum, maximum and standard deviation amount of transaction values of each node pair.
- **GNN with temporal sequences learning.** We also compare GTEA with TGAT (Xu et al. 2020), a state-of-the-art representation learning scheme for temporal interaction graphs, which has shown to consistently outperform

¹Raw data can be downloaded from: <https://www.kaggle.com/xblock/ethereum-phishing-transaction-network>

Table 1: Dataset Summary

Dataset	# Nodes	# Edges	# Interactions	Labeled Node Avg. Degree	# Ground Truths	# Node Features	# Edge Features
Eth-Role	2,180,689	3,745,858	55,322,096	306387.1	445	23	5
Phishing-Small	1,329,729	2,161,573	6,794,521	80.2	3360	3	3
Phishing-Large	2,973,489	5,355,155	184,398,820	302.0	6165	3	3
Mobile-Payment	2,143,844	4,568,936	21,326,122	66.8	6688	68	4

various recent schemes in this category, e.g. GAT+T and GraphSAGE+T.

- **GTEA variants** are implemented with different sequence model. Specifically, the variants equipped with LSTM and Transformer are denoted by GTEA-LSTM and GTEA-Trans respectively. Besides, the variants contain **T2V** are denoted by GTEA-LSTM+T2V and GTEA-Trans+T2V respectively.

Experimental Setup

In our experiments, each dataset is randomly split into a training set (60%), a validation set (20%) and a test set (20%). All models are tuned on the validation set and we report the classification accuracy and macro F1 score on the test set. For a fair comparison, each model is tuned independently with grid search to find the optimal hyperparameter combination. Only the best performance of each model is reported in this paper. Detailed information including hyperparameters, network configurations and the training process can be found in the supplementary materials.

Experimental Results on Node Classification

Table 2 shows the performance of the proposed model as well as all other compared methods. Some key observations are summarized as follow:

Overall Performance We observe that different variants of GTEA perform well in all four datasets and GTEA-LSTM consistently outperforms all other methods in the experiments. Such quantitative results demonstrate the effectiveness of the proposed GTEA framework. Different from other methods that learn from only part of available information, GTEA captures pairwise interaction dynamics through a temporal sequence model and incorporates the learned edge embeddings using GNNs. By making full use of all available information (from node features, features of temporal events and the graph topology), and learn the relationships and dependencies among all these features efficiently, GTEA delivers better node classification performance over all the dataset under test.

An additional observation is that LSTM variants perform slightly better than that of the Transformer. This may owe to the step-wise time-series processing and the sophisticated gate mechanism. In contrast to the Transformer, which looks into the entire interaction sequence at one go, LSTM incrementally updates its hidden states using successive interaction information. This enables the LSTM variant to capture patterns with time continuousness and model more fine-

grained temporal dependencies for an edge, which leads to better performance. We also observe that in Eth-Role and Mobile-Payment dataset, GTEA variants with **T2V** outperform those without **T2V**. This implies that periodic and non-periodic temporal patterns captured by **T2V** can benefit the node classification task. On the contrary, the performance of GTEA-LSTM and GTEA-Trans outperform their corresponding **T2V** variants in Phishing-Small and Phishing-Large dataset. This may be due to the fact that periodic patterns are not highly correlated with phishing events, where **T2V** can only make limited effect.

Effect of Edge Features From Table 2, we can observe that different GTEA variants outperform ECCConv and EGNN, which both incorporate handcrafted edge features in their framework. In contrast, GTEA learns edge embeddings from pairwise interactions through a sequence model. The performance gap between GTEA and ECCConv/ EGNN demonstrates that learning edge embeddings automatically can substantially improve the performance on node classifications. We also observe that ECCConv/ EGNN is hard to dominate methods trained with only node features, especially in the Eth-Role dataset. This is because node features in Eth-Role are elaborately derived from interaction sequences (e.g., number of days the account have activity records and the amount of mining reward received by the accounts), which can be informative and discriminative in classification tasks. Even though, GTEA still yields a better performance over these methods in all datasets, which reflects that our model can extract useful patterns from interaction sequences and make full use of them to improve the performance.

Effect of Pairwise Relationships Modeling Among all models that incorporate temporal information, GTEA performs the best, which answers the Question#3. Note that in TGAT, interactions among a target node and all its neighbors are grouped as one single time-series, which ignores pairwise temporal patterns and mutual relationships. On the contrary, the proposed GTEA explicitly models relation dependencies for pairwise nodal interaction-event sequence. This enables GTEA to capture more informative patterns and be superior to other competitors.

Effect of Sparsemax Fig. 4 shows the comparisons when GTEA is equipped with Sparsemax or Softmax (i.e., without Sparsemax), where the former can usually achieve a better performance. By introducing sparsemax, unimportant neighbors and noises can be filtered out before aggregation,

Table 2: Node Classification Results

Datasets	Eth-Role		Phishing-Small		Phishing-Large		Mobile-Payment	
Metrics	Accuracy	Macro F1	Accuracy	Macro F1	Accuracy	Macro F1	Accuracy	Macro F1
XGBoost	0.9211	0.9164	0.8482	0.8481	0.8694	0.7573	0.7152	0.7152
GCN	0.8084	0.8145	0.9077	0.9077	0.9298	0.8683	0.7481	0.7480
GraphSAGE	0.9868	0.9857	0.9405	0.9405	0.9753	0.9569	0.7474	0.7472
GAT	0.9868	0.9857	0.9405	0.9405	0.9631	0.9375	0.7265	0.7264
APNP	0.9868	0.9857	0.9241	0.9241	0.9084	0.8338	0.7716	0.7716
ECCConv	0.9079	0.8875	0.9301	0.9300	0.8962	0.7926	0.7399	0.7399
EGNN	0.9605	0.9497	0.8839	0.8823	0.9465	0.9035	0.7549	0.7538
GTEA-ST	0.9737	0.9708	0.9673	0.9673	0.9777	0.9615	0.7519	0.7516
TGAT	0.9737	0.9708	0.9673	0.9673	0.9623	0.9344	0.7212	0.7212
GTEA-LSTM	0.9868	0.9857	0.9836	0.9836	0.9805	0.9668	0.7848	0.7847
GTEA-LSTM+T2V	1.0000	1.0000	0.9777	0.9777	0.9789	0.9640	0.7990	0.7990
GTEA-Trans	0.9737	0.9708	0.9851	0.9851	0.9801	0.9658	0.7676	0.7670
GTEA-Trans+T2V	0.9868	0.9857	0.9792	0.9792	0.9769	0.9603	0.7758	0.7758

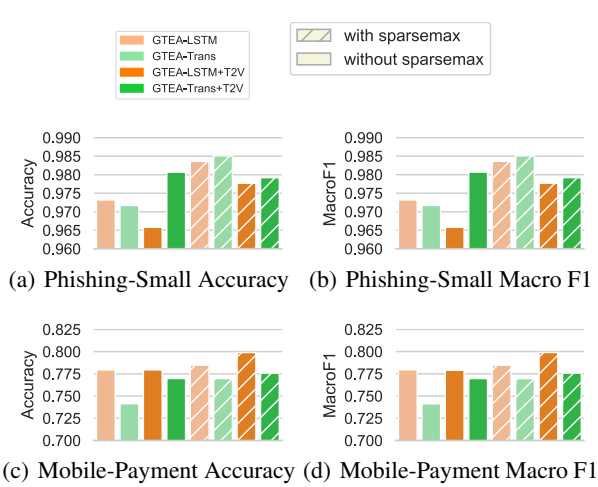


Figure 4: Ablation Study on Phishing-Small and Mobile-Payment Network dataset (with/ without sparsemax)

which yields more refined and discriminative embeddings that can benefit the classification task.

Effect of Temporal Learning without Node Features

Fig. 5 shows that the performance gap for all GTEA variants is much smaller. This implies that some critical information carried by handcrafted or derived interaction/ topology-related node features can be automatically learned by GTEA when generating edge embeddings. We also observe that the performance gap for GTEA is smaller than that of TGAT, which shows GTEA can learn the node representation better by capturing pairwise temporal patterns and relationships. These facts also demonstrate the advantages of GTEA over TGAT.

Conclusion and Future Work

In this work, we have presented GTEA - a new message passing mechanism which learns node and edge embed-

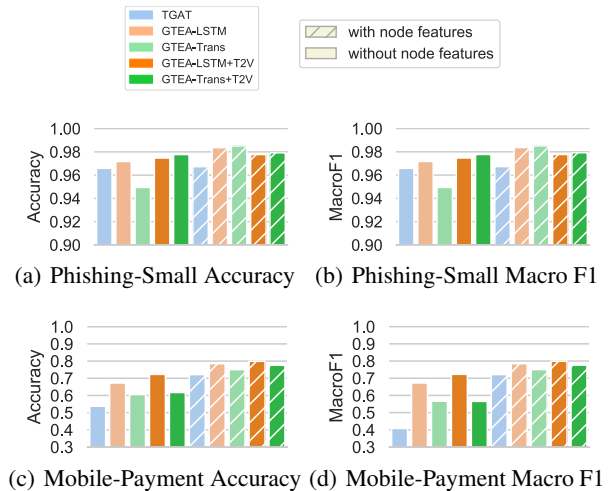


Figure 5: Ablation Study on Phishing-Small and Mobile-Payment Dataset (with/ without node features)

dings by exploiting the multi-dimensional, pairwise temporal patterns as well as complicated topological information in the temporal interaction graph. This method is designed to address the common drawbacks of existing representation learning methods for temporal interaction graph where complex temporal edge features and their interactions are either partially ignored or poorly supported. Empirical results show that GTEA consistently outperforms current state-of-the-art models. We also demonstrate that temporal edge features are important for node classification tasks. Ablation studies reveal that learning edge embeddings by the sophisticated neural sequence model with self-attention mechanism can give us better performance over static, handcrafted interaction-statistics-based features. Developing a more scalable, parallelized training platform for GTEA will be one promising direction for our future work.

References

- Chen, L.; Peng, J.; Liu, Y.; Li, J.; Xie, F.; and Zheng, Z. 2019. XBLOCK Blockchain Datasets: InPlusLab Ethereum Phishing Detection Datasets. <http://xblock.pro/ethereum/>.
- Chen, T.; and Guestrin, C. 2016. Xgboost: A scalable tree boosting system. In *Proceedings of the 22nd acm sigkdd international conference on knowledge discovery and data mining*, 785–794.
- Gong, L.; and Cheng, Q. 2019. Exploiting edge features for graph neural networks. In *Proceedings of the IEEE Conference on Computer Vision and Pattern Recognition*, 9211–9219.
- Grover, A.; and Leskovec, J. 2016. node2vec: Scalable Feature Learning for Networks. In *Proceedings of the 22nd ACM SIGKDD international conference on Knowledge discovery and data mining*, 855–864.
- Hamilton, W.; Ying, Z.; and Leskovec, J. 2017. Inductive Representation Learning on Large Graphs. In *Advances in neural information processing systems*, 1024–1034.
- Hochreiter, S.; and Schmidhuber, J. 1997. Long Short-term Memory. *Neural computation* 9(8): 1735–1780.
- Kingma, D. P.; and Ba, J. 2014. Adam: A method for stochastic optimization. *arXiv preprint arXiv:1412.6980*.
- Kipf, T. N.; and Welling, M. 2016. Semi-supervised Classification with Graph Convolutional Networks. *arXiv preprint arXiv:1609.02907*.
- Klicpera, J.; Bojchevski, A.; and Günnemann, S. 2018. Predict then propagate: Graph neural networks meet personalized pagerank. *arXiv preprint arXiv:1810.05997*.
- Kumar, S.; Zhang, X.; and Leskovec, J. 2019. Predicting dynamic embedding trajectory in temporal interaction networks. In *Proceedings of the 25th ACM SIGKDD International Conference on Knowledge Discovery & Data Mining*, 1269–1278.
- Li, Y.; Yu, R.; Shahabi, C.; and Liu, Y. 2018. Diffusion Convolutional Recurrent Neural Network: Data-Driven Traffic Forecasting. In *International Conference on Learning Representations (ICLR)*.
- Li, Z.; Zhang, L.; and Song, G. 2019. GCN-LASE: towards adequately incorporating link attributes in graph convolutional networks. *arXiv preprint arXiv:1902.09817*.
- Manessi, F.; Rozza, A.; and Manzo, M. 2020. Dynamic graph convolutional networks. *Pattern Recognition* 97: 107000.
- Martins, A.; and Astudillo, R. 2016. From softmax to sparsemax: A sparse model of attention and multi-label classification. In *International Conference on Machine Learning*, 1614–1623.
- Mehran Kazemi, S.; Goel, R.; Eghbali, S.; Ramanan, J.; Sahota, J.; Thakur, S.; Wu, S.; Smyth, C.; Poupart, P.; and Brubaker, M. 2019. Time2Vec: Learning a Vector Representation of Time. *arXiv preprint arXiv:1907.05321*.
- Pareja, A.; Domeniconi, G.; Chen, J.; Ma, T.; Suzumura, T.; Kanezashi, H.; Kaler, T.; Schardl, T. B.; and Leiserson, C. E. 2020. EvolveGCN: Evolving Graph Convolutional Networks for Dynamic Graphs. In *Proceedings of the Thirty-Fourth AAAI Conference on Artificial Intelligence*.
- Paszke, A.; Gross, S.; Massa, F.; Lerer, A.; Bradbury, J.; Chanan, G.; Killeen, T.; Lin, Z.; Gimelshein, N.; Antiga, L.; et al. 2019. PyTorch: An imperative style, high-performance deep learning library. In *Advances in Neural Information Processing Systems*, 8024–8035.
- Rahimi, A.; and Recht, B. 2008. Random Features for Large-scale Kernel Machines. In *Advances in neural information processing systems*, 1177–1184.
- Simonovsky, M.; and Komodakis, N. 2017. Dynamic Edge-conditioned Filters in Convolutional Neural Networks on Graphs. In *Proceedings of the IEEE conference on computer vision and pattern recognition*, 3693–3702.
- Singer, U.; Guy, I.; and Radinsky, K. 2019. Node Embedding over Temporal Graphs. In *Proceedings of the Twenty-Eighth International Joint Conference on Artificial Intelligence, IJCAI-19*, 4605–4612. International Joint Conferences on Artificial Intelligence Organization. doi:10.24963/ijcai.2019/640. URL <https://doi.org/10.24963/ijcai.2019/640>.
- Sitzmann, V.; Martel, J. N.; Bergman, A. W.; Lindell, D. B.; and Wetzstein, G. 2020. Implicit Neural Representations with Periodic Activation Functions. In *arXiv*.
- Trivedi, R.; Dai, H.; Wang, Y.; and Song, L. 2017. Know-evolve: Deep temporal reasoning for dynamic knowledge graphs. *arXiv preprint arXiv:1705.05742*.
- Trivedi, R.; Farajtabar, M.; Biswal, P.; and Zha, H. 2018. Dyrep: Learning Representations over Dynamic Graphs.
- Vaswani, A.; Shazeer, N.; Parmar, N.; Uszkoreit, J.; Jones, L.; Gomez, A. N.; Kaiser, Ł.; and Polosukhin, I. 2017. Attention is all you need. In *Advances in neural information processing systems*, 5998–6008.
- Veličković, P.; Cucurull, G.; Casanova, A.; Romero, A.; Lio, P.; and Bengio, Y. 2017. Graph Attention Networks. *arXiv preprint arXiv:1710.10903*.
- Wang, M.; Yu, L.; Zheng, D.; Gan, Q.; Gai, Y.; Ye, Z.; Li, M.; Zhou, J.; Huang, Q.; Ma, C.; et al. 2019. Deep graph library: Towards efficient and scalable deep learning on graphs. *arXiv preprint arXiv:1909.01315*.
- Xu, D.; Ruan, C.; Korpeoglu, E.; Kumar, S.; and Achan, K. 2020. Inductive Representation Learning on Temporal Graphs. *arXiv preprint arXiv:2002.07962*.
- Yan, S.; Xiong, Y.; and Lin, D. 2018. Spatial Temporal Graph Convolutional Networks for Skeleton-based Action Recognition. In *Thirty-second AAAI conference on artificial intelligence*.
- Yu, B.; Yin, H.; and Zhu, Z. 2018. Spatio-temporal Graph Convolutional Networks: A Deep Learning Framework for Traffic Forecasting. In *Proceedings of the 27th International Joint Conference on Artificial Intelligence (IJCAI)*.

Zhang, Z.; Bu, J.; Ester, M.; Zhang, J.; Yao, C.; Li, Z.; and Wang, C. 2020. Learning Temporal Interaction Graph Embedding via Coupled Memory Networks. In *Proceedings of The Web Conference 2020*, 3049–3055.

Supplementary Material

Dataset Description

Ethereum-Role Dataset This dataset is a multi-class role classification dataset based on the Ethereum Smart Contract network. Each type of account represents a special role in the Ethereum Payment System. Unlike Bitcoin, the address in Ethereum is an account which can be used repeatedly. We collect Ethereum transactions by using Google BigQuery and ground truth labels are collected from: <https://etherscan.io>. To build the graph, each account is taken as a node and transaction sequences between two nodes indicate an edge. The graph contains 2.18 million nodes, 55.3 million edges, and 443 labeled nodes with 7 types of users. 23 attributes (e.g. balance, in degree, etc.) and 5 interacting event (edge) attributes (e.g. timestamp, value, gas price, etc.) are extracted from the transaction records to be the raw node features.

Ethereum Phishing Datasets Ethereum Phishing Datasets are used for detecting phishing accounts in the Ethereum payment network. We collect two different Ethereum Phishing Datasets provided by (Chen et al. 2019), referred as *Phishing-Small* and *Phishing-Large* respectively². Graphs are constructed similar to the *Ethereum-Role* dataset. In *Phishing-Small*, we obtain 1,660 phishing nodes and 1,700 normal nodes. In *Phishing-Large*, 1,165 nodes are annotated as phishing and we randomly select 5,000 nodes from the rest as normal nodes, which sums up to 6,665 labeled nodes.

Mobile Payment Network Dataset With the rapid growth of mobile payment services, illicit users bring critical challenges to both service providers and regulators. We have collected a dataset, named as *Mobile-Payment*, from a major mobile payment provider, with 3347 users labeled as abnormal and 3341 normal users. We construct the graph by including neighbors of all labeled users and their corresponding transactions. Transactions between two users are represented as an edge, which corresponds to a sequences of their interaction events. After filtering out edges with small transaction count and nodes with large degrees, the resultant graph has 2,143,844 nodes and 21,326,122 edges. All user IDs are anonymized. All node and edge features, such as transaction amount, are normalized before experiments.

Experimental Setup

All the algorithms are implemented using Pytorch (Paszke et al. 2019) and DGL (Wang et al. 2019). For fair comparison, we tuned all baselines and GTEA variants with different hyperparameter settings. We search learning rate in $\{0.0001, 0.001, 0.01\}$, number of GNN layers in $\{1,$

$2, 3\}$, hidden embedding dimension in $\{32, 64, 128\}$ for both nodes and edges. Models using LSTM, i.e. our GTEA-LSTM and GTEA-LSTM+T2V, the number of temporal layers is searched from $\{1, 2, 4\}$. For Transformer-based variants, i.e. GTEA-Trans and GTEA-Trans+T2V, the number of transformer layers is selected among $\{1, 2, 3\}$, and the number of attention heads is set to 4. To enable training on large-scale graphs, we apply mini-batch training with neighbor sampling proposed by (Hamilton, Ying, and Leskovec 2017) for all models if applicable. We search the batch size in $\{32, 64, 128\}$, and the neighbors sampling size in $\{5, 10, 25\}$. Adam (Kingma and Ba 2014) is used as the optimizer in our training stage. We split the dataset into the train set (60%), validation set (20%), and test set (20%). For APPNP, we set the teleport (or restart) probability α to 0.1. We tuned the hyperparameters based on the validation set and we report the classification accuracy and macro F1 score on the test set. Our experiments are conducted on a single Linux machine with an AMD Ryzen Threadripper 3970X CPU @ 3.7GHz, 256 GB RAM, and two NVIDIA RTX TITAN GPUs with 24GB of RAM each.

²Raw data can be downloaded from: <https://www.kaggle.com/xblock/ethereum-phishing-transaction-network>